

EGU2020 – 6745: Session ERE 6.1

Coupled multiphase flow and geomechanics simulation of hydrate dissociation using FVM-FEM co-located variables arrangement

Rahul Samala and Abhijit Chaudhuri

Department of Applied Mechanics

IIT Madras

7 May 2020



Outline

- Introduction
- Governing equations
- Numerical methodology
- Validation
- Coupled flow and deformation
- Summary
- References

Introduction

- Gas hydrates are ice-like crystalline solids that form from mixtures of water and light natural gases. They have vast amount of trapped natural gas.



Methane hydrate structure and hydrate samples.

- Methane can be extracted from hydrates by depressurization. The dissociation of solid hydrate produces liquid water and methane gas.
- Dissociation of solid hydrates into fluid constituents weakens the strength bearing capacity of the sediment and can induce subsidence.
- The physical processes involved are hydrate phase change, non-isothermal multiphase flow, change in mechanical properties and strain field, and change in hydraulic properties.
- In this work a THMC coupled numerical solver is developed using node centered Finite volume method (FVM) for flow and Finite element method (FEM) for geomechanics. The state variables are hence co-located.
- The discretized equations are solved using PETSc, an open source suite of solvers.
- The pressure oscillations in numerical solution in the context of the choice of the numerical method - co-located variable arrangement along with unequal order function spaces for flow and displacement variables – and necessity of stabilization method is investigated.
- The performance of iterative coupled approach, where the flow and geomechanics equations are solved separately and sequentially, as against fully-coupled approach is also studied.

Governing Equations

- The mass balance equation for gas, water and hydrate phase ($\alpha = w, g$ and h)

$$\frac{\partial}{\partial t} (\phi \rho_{\alpha} S_{\alpha}) + \nabla \cdot (\phi \rho_{\alpha} S_{\alpha} \mathbf{v}_{\alpha,t}) = \dot{g}_{\alpha}$$

$$\text{where: } \phi S_{\alpha} \mathbf{v}_{\alpha,t} = \mathbf{v}_{\alpha} + \phi S_{\alpha} \mathbf{v}_s, \quad \mathbf{v}_{\alpha} = -\frac{kk_{r,\alpha}}{\mu_{\alpha}} (\nabla p_{\alpha} - \rho_{\alpha} \mathbf{g}), \quad \mathbf{v}_s = \frac{\partial \mathbf{u}}{\partial t}$$

\mathbf{v}_s is the solid velocity and \mathbf{u} is the displacement vector; $\mathbf{v}_h = 0$

- The soil mass balance equation is: $\frac{\partial}{\partial t} [(1 - \phi) \rho_s] + \nabla \cdot ((1 - \phi) \rho_s \mathbf{v}_s) = 0$

- The static equilibrium equation is: $\nabla \cdot \boldsymbol{\sigma} + \rho_{sh} \mathbf{g} = 0$

where ρ_{sh} is the density of the solid phase (soil and hydrate composite), and $\boldsymbol{\sigma}$ is the total stress.

- The stress-strain constitutive equation is:

$$\boldsymbol{\sigma} = 2G_m \boldsymbol{\epsilon} + \left(K_m - \frac{2}{3} G_m \right) (tr \boldsymbol{\epsilon}) \mathbf{I} - \alpha_b p_p \mathbf{I} - K_m \beta_{sh} (T - T_0) \mathbf{I}.$$

where, K_m, G_m are the bulk and shear modulus of the hydrate bearing medium.

β_{sh} and α_b are Biot coefficient and the thermal expansion coefficient.

- The energy equation is:

$$\frac{\partial}{\partial t} \left((1 - \phi) \rho_s U_s + \sum_{\alpha} (\phi \rho_{\alpha} S_{\alpha} U_{\alpha}) \right) + \sum_{\alpha} \nabla \cdot (\phi \rho_{\alpha} S_{\alpha} \mathbf{v}_{\alpha,t} H_{\alpha}) = \nabla \cdot (\lambda_{eff} \nabla T) + \dot{Q}^h.$$

U_{α}, H_{α} and λ_{eff} are internal energy, enthalpy of phase α and effective thermal conductivity.₄

Numerical Methodology

- The flow and energy equations are discretized using Finite volume method (FVM)
- The stress equilibrium equation is discretized using Finite element method (FEM)
- The discretized equations are solved using PETSc, an open source and parallel suite of routines for solving PDE and ODE.
- Point-centered or node centered FVM is used as it is easier to implement using PETSc.

➤ This choice of grid implies that the state variables for flow and geomechanics are **co-located**.

➤ The rate of change of volumetric strain term couples the flow and geomechanics equations.

➤ After calculating strain from the geomechanics solver (finite element mesh), it is interpolated to the finite volume mesh as

$$\varepsilon_{V_{ABCD}} = \frac{1}{4} \left(\frac{\varepsilon_{v_A} V_A + \varepsilon_{v_B} V_B + \varepsilon_{v_C} V_C + \varepsilon_{v_D} V_D}{V_{b_{ABCD}}} \right)$$

➤ The iterative coupled approach, where the flow and geomechanics equations are solved separately and sequentially, and fully-coupled approach, where all the equations are solved simultaneously are implemented.

➤ It is found that **unequal order function spaces** for flow and displacement alone cannot mitigate pressure oscillations for co-located variable arrangement, hence a physical influence scheme (PIS) stabilization method (Honorio et al. 2018) is implemented to mitigate it.

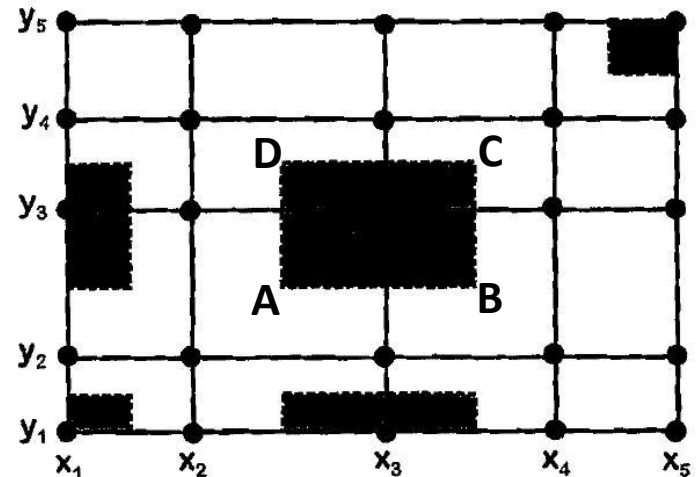


Fig 1: Point centered grid showing the corresponding control volumes (shaded area).

Validation

Flow code validation (Thermo-Hydro-Chemical, THC coupling)

The flow code is validated against experimental results of Tang et al. (2007), a cylindrical pressure vessel insulated and impermeable at one end and depressurized at the other end.

Parameter	Value
Length	50 cm
Cross-sectional area	11.4 cm ²
Porosity	0.308
Absolute Permeability	300 mD
Initial pressure	3.535 MPa
Initial water saturation	0.2961
Initial hydrate saturation	0.2183
Initial Temperature	1.54 °C
Boundary Pressure	0.93 MPa
Boundary Temperature	1.54 °C

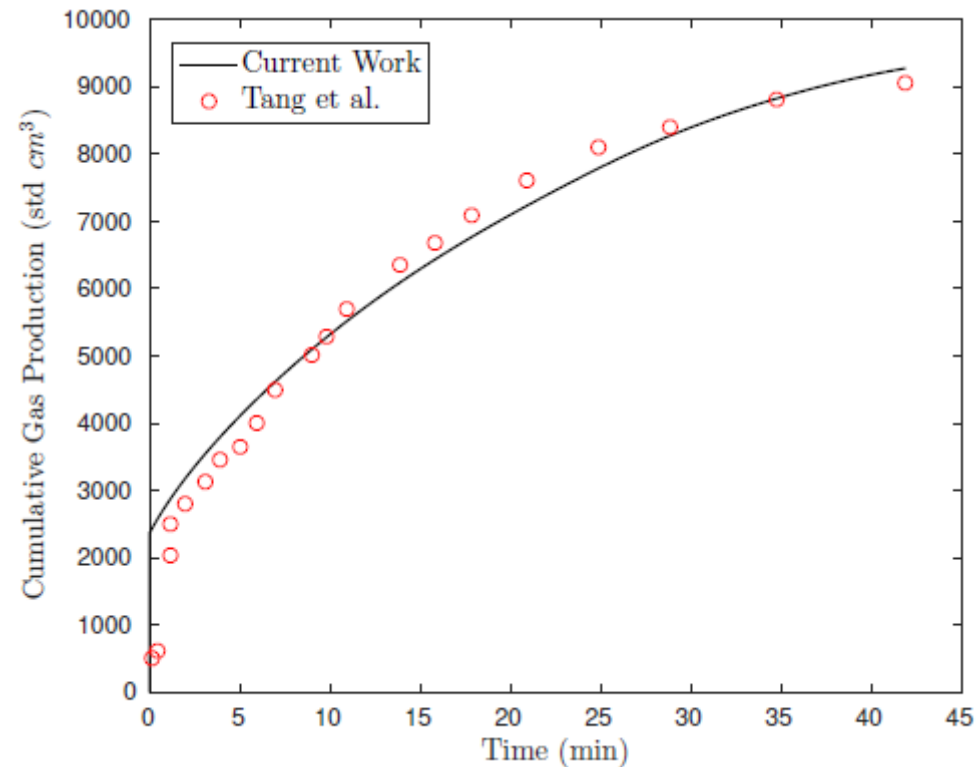


Fig 2: Cumulative gas production rate vs Time.

Validation

Geomechanics validation (Hydro-Mechanics, HM coupling)

The geomechanics code is validated against the analytical solution of the Mandel's problem.

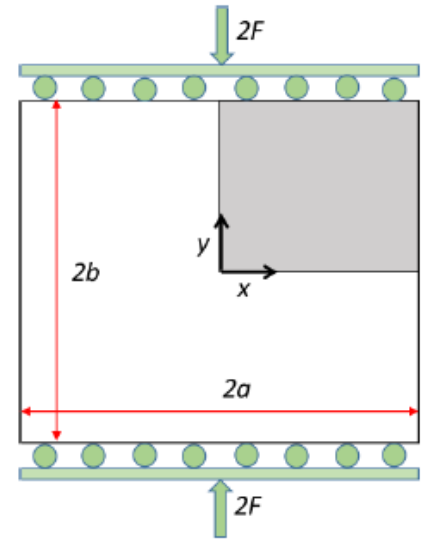
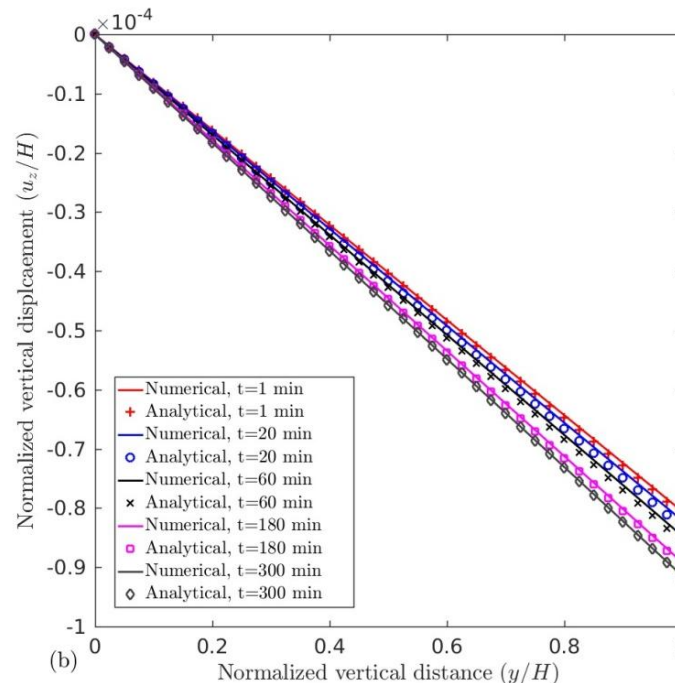
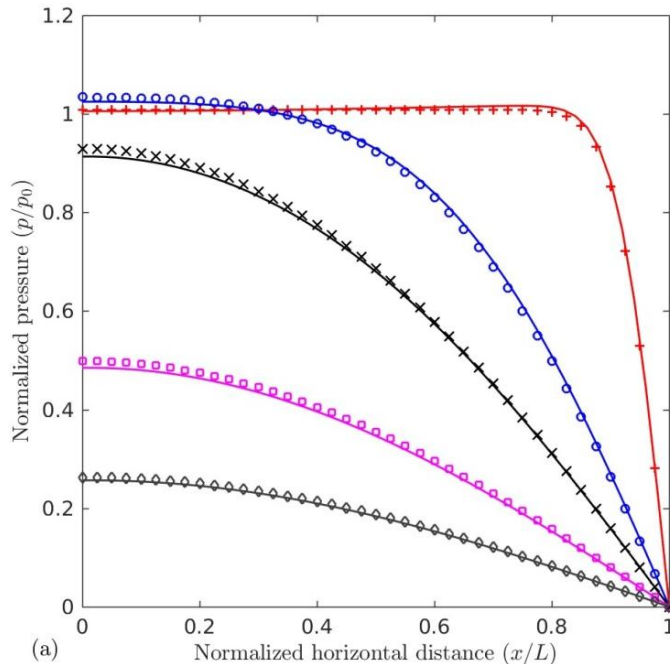


Fig 3: Mandel's problem configuration



Comparison of numerical and analytical solutions at various times:

(a) Non-dimensional pressure vs non-dimensional horizontal distance.

(b) Non-dimensional vertical displacement vs non-dimensional vertical distance.

Coupled hydrate dissociation and deformation

Hydrate Dissociation in layered systems with different permeability

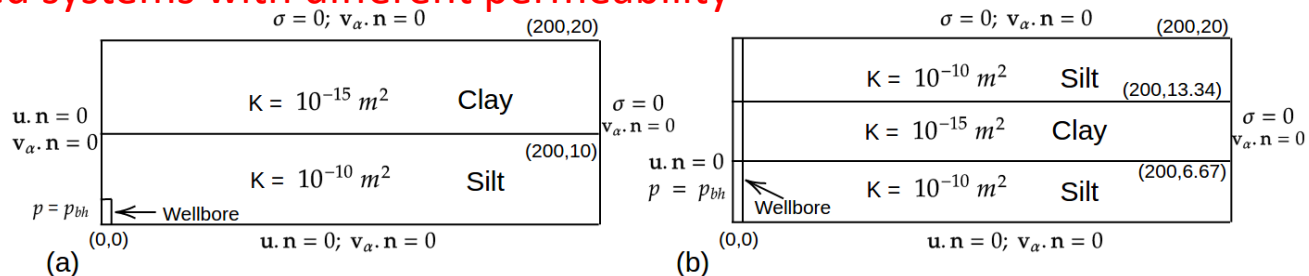


Fig 5: (a) Two layers with well bore penetrating small part of lower layer (b) Three layer system with well bore through out.

- Permeability variation is 5 orders of magnitude.
- PIS (Honorio et al. 2018) stabilization mitigates pressure oscillations.

Parameter	Value
Porosity	0.308
Absolute Permeability	Clay – $10^{-15} m^2$ Sand - $10^{-10} m^2$
Initial pressure	6.913 MPa
Initial water saturation	0.3
Initial hydrate saturation	0.6
Initial Temperature	283.15 K
Biot Coefficient	0.8
Poisson's Ratio	0.15
Young's Modulus	260 MPa
Well bottom hole pressure	4 MPa

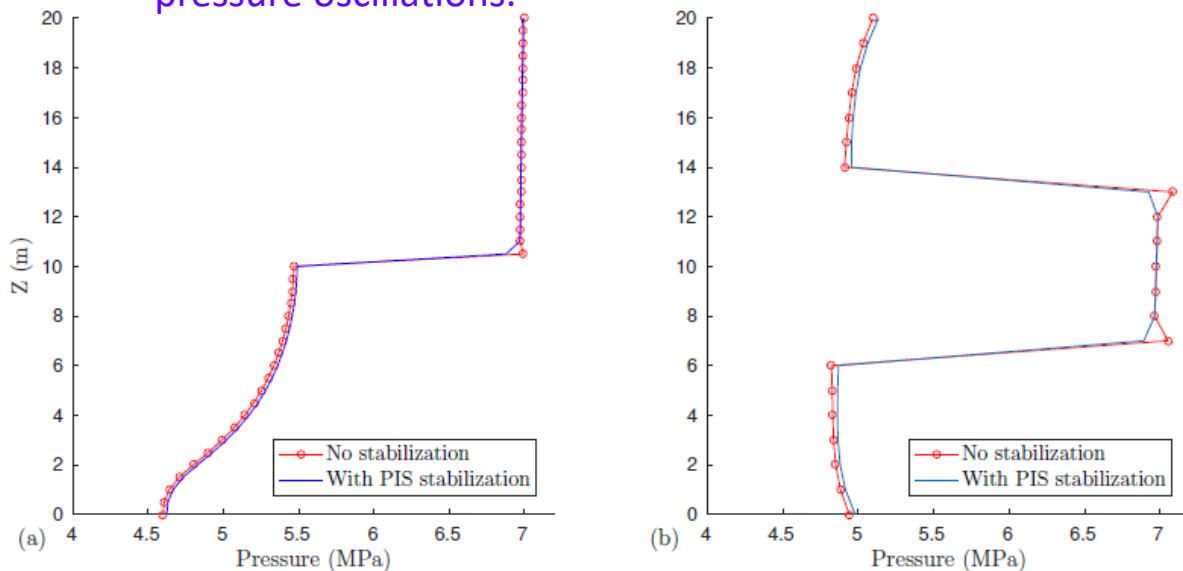


Fig 6: Comparison of pressure profiles near well bore with and without stabilization at $t=1 s (\Delta t=0.1 s)$ (a) domain with two layers (b) domain with three layers.

Coupled hydrate dissociation and deformation

Hydrate Dissociation: Comparison of iterative and fully-coupled solvers.

- Computational time for fully coupled solver is 1539 s and for the iterative solver is 760s for 5 hours of well operation.

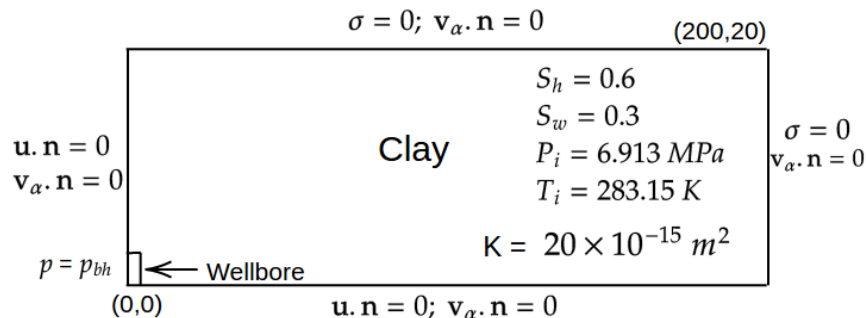


Fig 7: 2D domain for coupled dissociation and deformation problem.

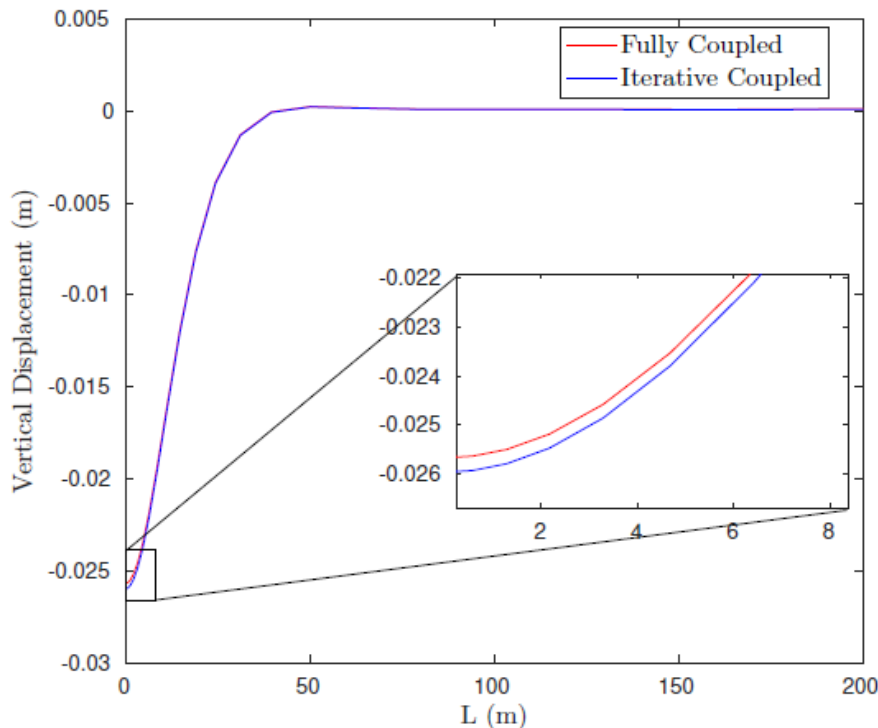


Fig 8: Comparison of iterative and fully-coupled solvers after 5 hours of well operation.

Summary

- A robust and efficient numerical THMC solver using PETSc routines was developed for gas hydrate dissociation with deformation.
- A node centered FVM for flow and FEM for geomechanics, that is, a co-located variable approach has been used.
- Unequal order function spaces for pressure and displacement along with co-located variable arrangement could not mitigate numerical pressure oscillations occurring at early times of simulation.
- PIS based stabilization scheme could mitigate the numerical pressure oscillations.
- The iteratively coupled approach is faster than the fully coupled approach due to smaller matrix size.

References

1. Hill, R., 1963. Elastic properties of reinforced solids: some theoretical principles. *Journal of the Mechanics and Physics of Solids* 11, 357–372.
2. Dvorkin, J., Prasad, M., Sakai, A., Lavoie, D., 1999. Elasticity of marine sediments: Rock physics modeling. *Geophysical Research Letters* 26, 1781–1784.
3. Honorio, H.T., Maliska, C.R., Ferronato, M., Janna, C., 2018. A stabilized element-based finite volume method for poroelastic problems. *Journal of Computational Physics* 364, 49 – 72.
4. Tang, L.G., Li, X.S., Feng, Z.P., Li, G., Fan, S.S., 2007. Control mechanisms for gas hydrate production by depressurization in different scale hydrate reservoirs. *Energy & Fuels* 21, 227–233.